

The *polycotyledon* Mutant of Tomato Shows Enhanced Polar Auxin Transport¹

Arif S.A. Al-Hammadi², Yellamaraju Sreelakshmi², Sangeeta Negi, Imran Siddiqi, and Rameshwar Sharma*

School of Life Sciences, University of Hyderabad, Hyderabad-500046, India (A.S.A.A.-H., Y.S., S.N., R.S.); and Center for Cellular and Molecular Biology, Tarnaka, Uppal Road, Hyderabad-500007, India (I.S.)

The *polycotyledon* mutant of tomato (*Lycopersicon esculentum* L. cv Ailsa Craig) showed altered development during embryogenesis and during vegetative and reproductive phases. The phenotype was pleiotropic and included the formation of extra cotyledons, changes in leaf shape, increased number of flowers (indeterminacy) with abnormal floral organs, the formation of epiphyllous structures, and altered gravitropism. The earliest defects were observed at the transition from the globular to the heart stage of embryogenesis with the formation of multiple cotyledons. Epidermal cells in the mutant embryo were smaller and less expanded compared with wild type. Examination of polar auxin transport (PAT) showed a striking enhancement in the case of the mutant. Increase in PAT did not appear to be caused by a decrease in flavonoids because the mutant had normal flavonoid levels. Application of 2,3,5-triiodobenzoic acid, an inhibitor of polar transport of auxin, rescued postgermination phenotypes of young seedlings. Our analysis reveals a level of control that negatively regulates PAT in tomato and its contribution to plant development and organogenesis.

In higher plants, phytohormone auxin (indole-3-acetic acid [IAA]) is transported basipetally from its site of synthesis at the shoot apex toward the roots by a process termed polar auxin transport (PAT). PAT provides directional information regulating several facets of plant development such as cell elongation, vascular differentiation, apical dominance, tropic movements, and organ development (Lomax et al., 1995). Physiological studies have indicated that PAT requires specific auxin influx and efflux carriers located on the plasma membrane of transporting cells. Biochemical studies support a "chemiosmotic model" of auxin transport that proposes that uncharged, protonated auxin can enter cells from the acidic apoplast either passively by diffusion or via energized uptake by specific influx carriers. In the cytosol because of the more basic pH, IAA is deprotonated and is trapped within the cell due to poor membrane permeability of anion. As a consequence, anionic IAA can leave the cell only by the action of auxin efflux carriers (Rubery and Shelldrake, 1974; Raven, 1975). The polarity of auxin transport presumably is maintained by localization of auxin efflux carrier molecules at the basal ends of transporting

cells (Jacobs and Gilbert, 1983). The selective efflux of auxin anion from the basal ends of transporting cells and arrangement of these cells in a long file from the shoot apex to the root apex is the basis of PAT.

Much of our current knowledge about the nature of components participating in PAT comes from molecular genetic analysis of mutants of Arabidopsis that are defective in transport of auxin. The *pin1* mutant has reduced PAT, characteristically develops a naked pin-like inflorescence, and shows morphological abnormalities in flowers and leaves. The *PIN1* gene encodes a membrane protein that most likely functions as an auxin efflux carrier as suggested by its localization at the basal ends of xylem parenchyma cells in vascular bundles (Gälweiler et al., 1998). Another group of mutants defective in the *pin2/agr1/eir1/wav6* locus displays agravitropic roots and reduced root growth and exhibits a defect in auxin transport in roots. The product of the *EIR1/AGR1/PIN2/WAV6* gene shows similarities to *PIN1* protein and is asymmetrically localized at the periclinal side of epidermal and cortical cells in the meristematic region and elongation zone of the root (Chen et al., 1998; Luschignig et al., 1998; Müller et al., 1998). Similar to *pin1*, the *pid1* mutant also shows reduced PAT and produces a naked inflorescence devoid of floral buds (Bennett et al., 1995). *PID1* encodes a Ser-Thr protein kinase that was initially proposed to have a signaling or regulatory function in auxin action (Christensen et al., 2000) and appears to act as a positive regulator of auxin transport (Benjamins et al., 2001). A similar link between auxin transport and protein phosphatase 2A is seen in the *rcn1* mutant, which shows root curling in the presence of 1-naphthylphthalamic acid (NPA; Rashotte et al., 2001). The *aux1* mutant is de-

¹ This work was supported by the government of Yemen (fellowship to A.S.A.A.-H.), by Council of Scientific and Industrial Research (CSIR; fellowships to Y.S. and S.N. and grant to R.S.), by International Atomic Energy Agency (IAEA; grant to R.S.), and by Department of Science and Technology (DST; grant to R.S.).

² These authors contributed equally to the paper.

* Corresponding author; e-mail rpsl@uohyd.ernet.in; fax 0091-40-23010120.

Article, publication date, and citation information can be found at <http://www.plantphysiol.org/cgi/doi/10.1104/pp.103.025478>.

fective in auxin uptake and displays defects in gravitropic responses and resistance to exogenous auxin (Pickett et al., 1990). The *AUX1* gene encodes an influx carrier of auxin that has characteristics of an amino acid permease-like protein (Bennett et al., 1996; Marchant et al., 1999).

The treatment of plants with inhibitors of auxin efflux carrier activity, 2,3,5-triiodobenzoic acid (TIBA) and NPA, influences many growth and developmental processes thought to be controlled by PAT. The *pin1* phenotype could be copied in wild-type Arabidopsis by treatment with auxin transport inhibitors with alterations in vascular development and the formation of a pin-like inflorescence instead of floral buds (Okada et al., 1991; Gälweiler et al., 1998). It has been proposed that NPA acts by binding to a plasma membrane-associated protein called the NPA-binding protein (Muday et al., 1993; Bernasconi et al., 1996). Evidence suggests that NPA-binding protein is distinct from the auxin efflux carrier and plays an important role in cycling of auxin efflux carriers to plasma membranes (Geldner et al., 2001). The *tir3* mutants that are resistant to the inhibitory action of NPA on root elongation show a pleiotropic phenotype, including reduced inflorescence height with few and short siliques, decreased petiole and root length, and reduced apical dominance (Ruegger et al., 1997). The *TIR3* gene, renamed *BIG*, encodes a protein that might be essential for proper positioning of PIN1 at the plasma membrane (Gil et al., 2001).

Several lines of physiological evidence have suggested that a specific class of flavonoids may act as auxin transport inhibitors (Jacobs and Rubery, 1988). Flavonoids such as quercetin act as competitive inhibitors of NPA binding, suggesting both compounds may regulate auxin transport by binding to the same protein (Murphy et al., 2000). The flavonoid-deficient *tt4* mutant shows reduced inflorescence length, reduced apical dominance, increased root branching, and stimulation of basipetal transport of auxin in inflorescence segments (Brown et al., 2001).

A distinct role for PAT has been noticed during plant embryogenesis, particularly in cotyledon development. It is observed that auxin transport is necessary for the establishment of bilateral symmetry during the transition from the globular to heart stage of embryogenesis leading to formation of cotyledons (Liu et al., 1993; Hadfi et al., 1998). The treatment of excised globular mustard (*Brassica juncea*) embryos with inhibitors of PAT caused fusion of cotyledons at the subsequent heart stage (Liu et al., 1993). During wild-type embryogenesis, PIN1 shows polar localization beginning at the mid-globular stage with localization narrowing down to vascular precursor cells in the cotyledonary primordia and embryo axis, whereas the *gnom* mutant that shows disorganized localization of PIN1 in globular embryos fails to develop cotyledonary primordia (Steinmann et al.,

1999). Apparently, GNOM localizes to endosomes where it controls the polarized trafficking of PIN1 to the basal plasma membrane (Geldner et al., 2003). In the *gnom* mutant, PIN1 accumulates internally and fails to localize to the plasma membrane, causing the mutant phenotype.

Little information is available on mutants defective in auxin action/transport in species other than Arabidopsis. The *dgt* mutant of tomato (*Lycopersicon esculentum* L. cv Ailsa Craig) has been reported to be defective in auxin action, and its phenotype can be ascribed to reduced sensitivity of mutant tissues to auxin (Kelly and Bradford, 1986; Muday et al., 1995; Coenen et al., 2003). In this report, we show that the *poc* (*polycotyledon*) mutation in tomato enhances PAT. The mutant displays several developmental abnormalities throughout the life cycle of the plants, from embryonic to vegetative and reproductive phases, suggesting that these changes may be related to alteration of auxin transport in the mutant. We also show that the postgermination seedling phenotype of the mutant can be rescued by treatment with TIBA consistent with the view that this is due to enhanced PAT.

RESULTS

Genetic Characterization of the Polycot Mutant

The *polycot* mutants were initially identified based on their abnormal seedling phenotype highlighted by the presence of extra cotyledons. The mutants were male sterile due to the lack of dehiscence of the anther sac; nevertheless the anther sacs contained viable pollens (75%–80% germination). As a consequence, the mutant was maintained in homozygous state by manual self-pollination. The crosses with wild type yielded normal F₁ seedlings with the wild-type phenotype in seedling stage and during vegetative and reproductive development and were self-pollinating with normal setting of seeds. The genetic segregation analysis of F₂ seedlings showed that the mutant phenotype was inherited as a monogenic Mendelian trait (119 seedlings, wild type; 42 seedlings, polycot). The reciprocal crosses with wild type also showed 3:1 segregation of wild type and *poc* phenotype in F₂ generation. The above segregation analysis suggests that the *poc* mutant contains a monogenic, recessive, and nuclear mutation. Though we obtained nine mutant lines, the results of complementation analysis using homozygous *poc* lines showed that all these lines were allelic, showing only the *poc* phenotype in the F₁ generation. This was further supported by the results of crossing with heterozygous *poc* lines. The F₁ progeny of these lines segregated in typical 3:1 ratio of wild-type and *poc* seedlings (data not shown). Given the ratio of M₂:M₁ plants (50,000:1,500), these results are consistent with the view that the above nine lines of *poc* mutants likely represent siblings. One line was named *poc1-1*

and backcrossed twice for further characterization. The crossing of *poc* mutants with the *Ds* transposon-tagged *dem* mutant (Keddie et al., 1998), which also has a variable number of cotyledons, revealed lack of allelism between these two mutants (M. Kavitha, M.S. Sharada, P. Janila, S. Negi, R. Sharma, unpublished data).

The *poc* Mutant Shows Pleiotropic Developmental Defects

Nearly all *poc* mutant seedlings (98.5%, $P > 0.0001$) showed extra cotyledons with approximately one-half of the seedlings being tetracot and about 35% seedlings being tricot. In the remaining seedlings, the cotyledons showed varied extent of fusion yielding tricot or dicot seedlings (Fig. 1A). The fused cotyledons could be distinguished from a normal single cotyledon by the presence of two midveins in the blade pointing toward the respective tips and running in parallel in the petiole (Fig. 1B). Though a minor number (1.5%) of seedlings showed a dicot phenotype, these could be distinguished from the wild type by their round-shaped cotyledons (Fig. 1C). The roots of *poc* seedlings were distinctly shorter than the wild type and showed earlier appearance of lateral roots, and in adult mutant plants, the roots were bushier than the wild type.

Nearly all *poc* mutant plants showed abnormalities in the shape and size of leaves. Based on the leaf abnormalities, we classified *poc* plants under three classes (Fig. 1D). The class A plants showed a short and bushy phenotype. Leaves of class A were shorter in size and bore smaller, narrow, and curled leaflets (Fig. 1E). A distinct feature of this class is the appearance of epiphyllous structures with a nearly 100% frequency resembling leaves and shoots on rachis normally near the junction to petiolules (Fig. 1F). The class B plants were only somewhat shorter than the wild type. Though the leaves of class B appeared similar to class A, the leaf size was intermediate between wild type and class A, and the leaflets were less curled than class A (Fig. 1E). Also, no epiphyllous structures were seen on class B leaves. The most severe abnormalities were observed in leaves of class C. The leaf lacked the small and minor leaflets, and the characteristic lobing of the blade was absent in the major leaflets (Fig. 1E). In extreme cases, the leaf lacked both small and minor leaflets and formed a lanceolate leaf. The loss of lobing in the leaflet margin was associated with an altered venation pattern of the leaflets with veins headed toward the leaflet tip. The formation of first inflorescence in class C is delayed, and it appears only after formation of the 16th node, whereas in wild type and in the other two classes of *poc* mutant, inflorescence forms between the eighth and 10th node.

In wild-type plants, the inflorescence consists of about seven to 14 flowers that are organized in a

simple cyme pattern. This pattern of organization in the inflorescence was disrupted in *poc* mutants, with appearance of multiple branches on the main axis of the inflorescence, which either terminated in a flower or dichotomously branched further to give additional flowers. The number of flowers in *poc* inflorescences ranged between 20 and 60, with about 50 flowers being more common (Fig. 1G). Markedly, in the *poc* inflorescence, most flowers bloomed at the same time.

The *poc* mutation showed incomplete penetrance for the observed floral abnormalities (Tables I and II); however, the penetrance for male sterility was nearly 100%. The *poc* mutants grown in the greenhouse or net house did not produce any fruit unless these were self-pollinated by hand. Several abnormalities were observed in *poc* floral organs such as increase in number, decrease in size, and fusion of organs (Fig. 1H). Many flowers also showed occasional formation of mosaic organs (Table II). The number of petals in *poc* mutant was higher, and petals were relatively short with petals of class C being smallest in size. In nearly one-half of the flowers, the petals developed an appendage of tissue facing toward stamens (Fig. 1I). In many flowers, this appendage penetrated between anther filaments, causing separation of stamens. Nearly two-thirds of flowers of the class C mutant flowers contained a patch of green tissue resembling sepals in the center of petals. Similarly, the sepals of *poc* flowers showed an increase in number and about 5% to 8% of flowers contained petaloid sepals with a sector of tissue resembling petals (Fig. 1J). Occasionally, the sepals were fused with neighbors, with highest fusion (94%) in the flowers of class C.

The characteristic fusion of stamens resulting in the formation of a narrow-necked anther tube was nearly absent in the *poc* flowers (Fig. 1K). The flowers of the *poc* mutant were male sterile because the anthers lacked dehiscence. In class B and C flowers, the stamens were twisted, distorted, and also variable in size. In class C, the stamen number was reduced, and stamens were fused to the carpels (Fig. 1L). Despite these severe abnormalities, the gynoecium of these flowers remained functional. Occasionally, from within a fully differentiated *poc* flower, either an inflorescence bearing flowers (Fig. 1M) or a shoot developed. Several of these phenotypes are indicative of the floral meristem retaining features of the inflorescence and may reflect an incomplete transition from the inflorescence to a floral meristem.

Multiple Cotyledons Initiate at the Heart Stage in Mutant Embryos

The appearance of multiple cotyledons in *poc* seedlings is a manifestation of the alteration of embryo development in the mutant. Growth of the embryo in the *poc* mutant was slower than in the wild type. At

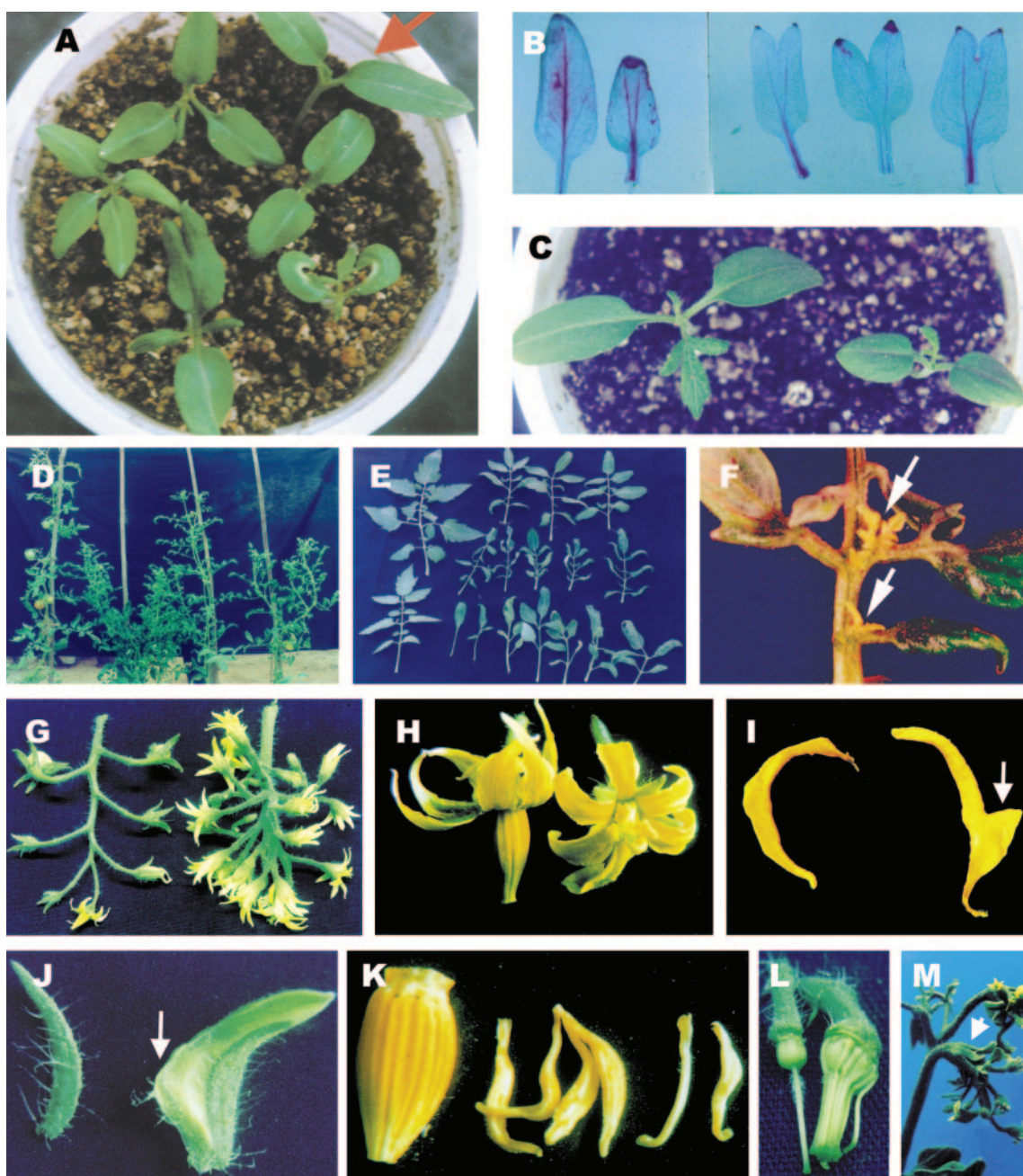


Figure 1. Morphology of *poc* plants throughout life cycle. A, *poc* seedlings (clockwise from top right): wild-type seedlings (arrow); dicot [1+(2)], note two midveins; dicot with two halves of curled cotyledons; dicot [1+(2)] with a partially fused cotyledon; tetracot; and tricot. B, Fused *poc* cotyledons showing two midveins running parallel in the petiole. Wild type (left). C, *poc* dicot seedling showing smaller and more rounded cotyledons. Wild type (left). D, Phenotype of 3.5-month-old plants. Wild type (left), *poc A* (second from left), *poc B* (third from left), *poc C* (right). E, Adult leaves (sixth node onwards) of 3-month-old wild type and *poc* mutant. In *poc* mutant, the leaf abnormalities vary from the simple lanceolate leaf to leaf with variable number of leaflets, reduction in size, and loss of lobing in leaflets. Wild type (upper and lower left), *poc B* (upper row), *poc A* (middle row), *poc C* (lower row). Wild-type leaves (upper and lower left). F, Epiphyllous structures (arrows) on *poc* leaves appearing near the junction of petiolule to the rachis. G, *poc* inflorescence (right) showing multiple blooming flowers with abnormal phyllotactic arrangement. H, *poc* flower (right) showing the absence of anther cone and shorter petals. I, *poc* petal (right) with an appendage on stamen-facing side (arrow). J, *poc* sepal (right) with a petal-like sector. Note the absence of trichomes (arrow). K, Twisted and short stamens of *poc* mutant lacking fusion to form anther cone. Wild type (left). L, Fusion of stamens of *poc* to the carpel. M, Appearance of a new inflorescence from inside of a fully differentiated flower of *poc* mutant (arrow).

Table I. The no. and length of floral organs in wild type (WT) and *poc* mutant

The sample size was 50 flowers from each genotype WT, *poc* A, *poc* B, and *poc* C. The *P* values (WT versus mutant) were calculated using a two-tailed Student's *t* test as described in "Materials and Methods." The *P* values for all mutant samples were less than 0.0001.

Organ	No. of Organs				Length of Organs (mm)			
	WT	<i>poc</i> A	<i>poc</i> B	<i>poc</i> C	WT	<i>poc</i> A	<i>poc</i> B	<i>poc</i> C
Sepals	6.32 ± 0.12	7.42 ± 0.1	7.26 ± 0.14	7.44 ± 0.15	6.84 ± 0.18	5.1 ± 0.12	6.06 ± 0.15	5.86 ± 0.22
Petals	5.98 ± 0.099	7.14 ± 0.097	6.85 ± 0.14	6.92 ± 0.14	11.32 ± 0.21	9.72 ± 0.195	10.82 ± 0.22	8.48 ± 0.22
Stamens	6.04 ± 0.09	7.04 ± 0.08	6.84 ± 0.13	5.4 ± 0.16	8.28 ± 0.14	7.38 ± 0.14	7.9 ± 0.13	6.08 ± 0.18
Carpels	2.12 ± 0.15	2.5 ± 0.08	2.62 ± 0.12	Not observed	7.26 ± 0.13	6.4 ± 0.14	7.56 ± 0.12	5.2 ± 0.18

10 d after pollination (DAP), the globular embryo of the mutant was approximately 60% the size of the wild-type embryo (Fig. 2, A and B). The *poc* embryo was smaller at the late globular stage (Fig. 2, C and D). The slower development of *poc* embryos was apparent at the triangular stage, where the *poc* embryo was shorter and squatter in shape relative to the wild type (Fig. 2, E and F). The central procambium region of the *poc* embryo was also broader at this stage (Fig. 2, E and F). A comparison of cell shape in the medial epidermis of the *poc* embryo revealed that the cells were more square in shape in comparison with wild type, in which cells were more rectangular and elongated along the anticlinal axis (Fig. 2, I and J). In fact, *poc* embryos do not show a typical heart stage because in place of two cotyledons, three or four cotyledons form in the embryo (Fig. 2, G and H).

Cell Size Is Altered in the *poc* Mutant

A decrease in size of cells in the *poc* mutant was noticed for developing embryos at the triangular stage. Scanning electron microscopy (SEM) examination of the surface of cotyledons and hypocotyls showed a similar change in cell size in the mutant seedlings. The increase in cotyledon number was associated with a reduction in size of epidermal cells of cotyledons and hypocotyls for *poc*. The abaxial epidermal cells of wild-type cotyledons (Fig. 3A) were larger in size ($2,396 \pm 107.3 \mu\text{m}^2$) than the *poc*

mutant cells ($2,050 \pm 74.3 \mu\text{m}^2$, $P = 0.0380$; Fig. 3B). A similar difference in width was also visible in epidermal hypocotyl cells of light-grown plants, between wild type ($23.94 \pm 0.7 \mu\text{m}$) and *poc* ($15.13 \pm 0.61 \mu\text{m}$, $P = 0.0007$; Fig. 3, C and D).

PAT Is Enhanced in the *poc* Mutant

The transport of [^{14}C] IAA was monitored in stem segments in both the acropetal and basipetal directions using two different methods outlined by Okada et al. (1991) and Daniel et al. (1989; Fig. 4, A and B). Using both of these methods, it was found that the polar transport of auxin in *poc* mutant was significantly higher than the wild-type control. In the acropetal direction, transport of auxin was minimal and about the same in wild type and mutant. In contrast, a significant increase in auxin flow was observed in the basipetal direction with the *poc* mutant displaying nearly 2.5- to 3-fold higher transport than the wild type. The inclusion of TIBA reduced the magnitude of transport in both mutant and wild type. In an assay for retention of auxin, the *poc* mutant displayed decreased accumulation of auxin as evident by less retention of [^{14}C] IAA as compared with wild type (Fig. 4C). The fact that inclusion of TIBA increased the amount of retention of [^{14}C] IAA indicates the process to be mediated by PAT. The possibility that enhanced PAT could be due to a reduction in flavonoid levels is argued against by the observation that both *poc* mutant (0.70 ± 0.11 , A_{330}/shoot , $P = 0.7071$) and wild type (0.64 ± 0.10 , A_{330}/shoot) plants have similar levels and spectra of flavonoids (Fig. 4D).

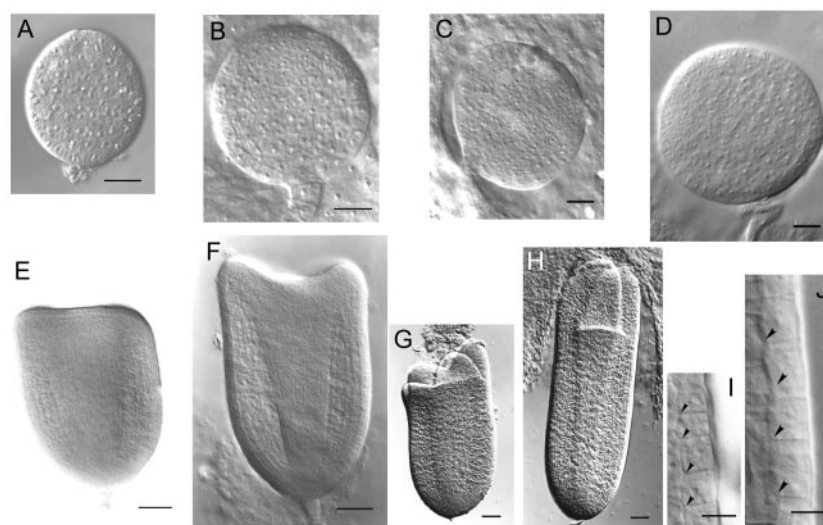
The Seedling Phenotype of *poc* Can Be Rescued by TIBA

The hypocotyls of dark-grown *poc* seedlings were distinctly shorter than those of wild type (Fig. 5A). In view of enhanced PAT in the mutant, we reasoned that faster PAT might deplete auxin levels in hypocotyl cells, leading to the observed phenotype. In that case, a reduction in PAT by application of TIBA should rescue the phenotype of *poc* seedlings. The observed increase in length of hypocotyls of dark-grown *poc* seedlings at a low concentration of TIBA supports this presumption (Fig. 5A). TIBA at a wide

Table II. The frequency of floral organ abnormalities in the flowers of different classes of *poc* mutant ($n = 150-200$)

Phenotypic Abnormalities	Mutant Class		
	<i>poc</i> A	<i>poc</i> B	<i>poc</i> C
	%		
Organ fusion			
Fusion of sepals	5	5	94
Lack of fusion of stamens	85	75	100
Stamens fused to carpels	0	0	89.4
Petals and stamens fused to carpels	0	0	3
Identity change			
Petaloid sepals	7.5	7.5	5.3
Outgrowth in petals	52.5	22.5	60
Sepaloid petals	0	2.5	65.8
White-green petals	0	2.5	5.3

Figure 2. Comparison of the development of embryo in *poc* mutant (A, C, E, G, and I) and wild-type plants (B, D, F, H, and J). A and B, Globular stage 10 DAP. C and D, Late globular stage (13 DAP). E and F, Triangular/early heart stage (15 DAP). G and H, Late heart/torpedo stage (18 DAP). I and J, Magnification of medial epidermal cells from the right-hand margin region of embryos shown in E and F, respectively. Arrowheads, Cell boundaries in an epidermal cell file. Scale bars: A to D, 10 μm ; E to G, 20 μm ; and I and J, 5 μm .



range of concentrations tested (0.1–10 μM) brought about a stimulation of hypocotyl elongation in the mutant relative to the untreated control. At 0.3 μM concentration, TIBA promoted elongation of the *poc* hypocotyls by 43%, compared with a minor 10% reduction in wild type (Fig. 5C). At 10 μM , hypocotyls were 18% longer than untreated seedlings in the case of the mutant, whereas wild type showed a 22% reduction relative to the untreated control.

The root length of light-grown *poc* seedlings was nearly 3 times less than the wild type (Fig. 5B), but root tip is normal as visualized by amyloplast staining (Benjamins et al., 2001). The possible relationship of the short root phenotype with enhanced PAT in the *poc* mutant was examined by application of TIBA. The inclusion of 0.5 μM TIBA could fully restore the *poc* root length to a level similar to that of the wild type. Interestingly, this low concentration of TIBA had no significant effect on the length of wild type roots (Fig. 5D). For roots, as for hypocotyls, TIBA-

mediated stimulation of elongation was seen for a wide range of concentrations (0.1–10 μM).

The response to auxin was normal in roots of *poc* seedlings as evidenced by similarity to wild type for auxin-mediated inhibition of root elongation (Fig. 5E). The inhibitory action of auxin also indicates that reduced elongation of *poc* roots might be due to overaccumulation of auxin. The possibility that shorter hypocotyl length of dark-grown mutant seedlings resulted from auxin deficiency was examined by studying elongation of excised hypocotyls in the presence of auxin. Although auxin only slightly stimulated elongation of wild type, it significantly stimulated elongation of mutant hypocotyl (Fig. 5F), indicating a likely deficiency of auxin in the mutant tissue. Taken together, these data show that several of the phenotypes of the *poc* mutant can be ascribed to a depletion of auxin arising from increased PAT and not to a reduced sensitivity to auxin because the mutant retains substantial sensitivity to exogenously applied auxin.

Examination of transverse sections of *poc* hypocotyls revealed alteration in anatomy, particularly with respect to vascular differentiation (Fig. 6). In wild-type seedlings, the vascular bundles were usually arranged as four bundles (two pairs of two bundles) with a central pith. A distinct feature of the *poc* mutant was that vascular bundles were arranged near each other due to a reduction in the central pith region (Fig. 6C). Chemical inhibition of the PAT in *poc* seedlings resulted in proliferation of xylem vessels with appearance of central pith and arrangement of bundles similar to untreated wild-type control (Fig. 6D). In contrast, in the presence of TIBA, the proliferation of xylem vessels in wild type led to fusion of adjacent bundles (Fig. 6B). These results indicate that changes in the vasculature of the *poc* mutant could be due to altered levels of auxin.

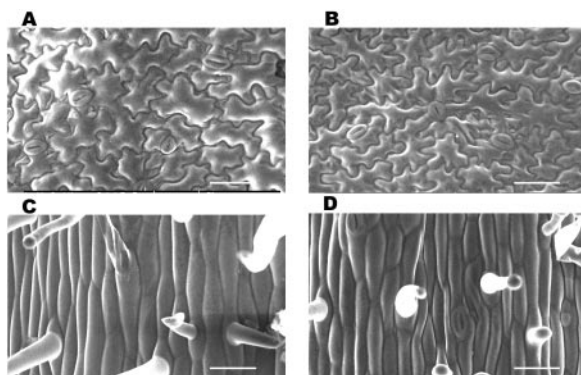


Figure 3. Scanning electron micrograph of epidermal cells of light-grown seedlings. A and B, One-week-old cotyledons showing that the *poc* (B) has smaller cells. C and D, One-week-old hypocotyls showing that *poc* (D) have shorter and less broad cells. Scale bars in A to D: 50 μm .

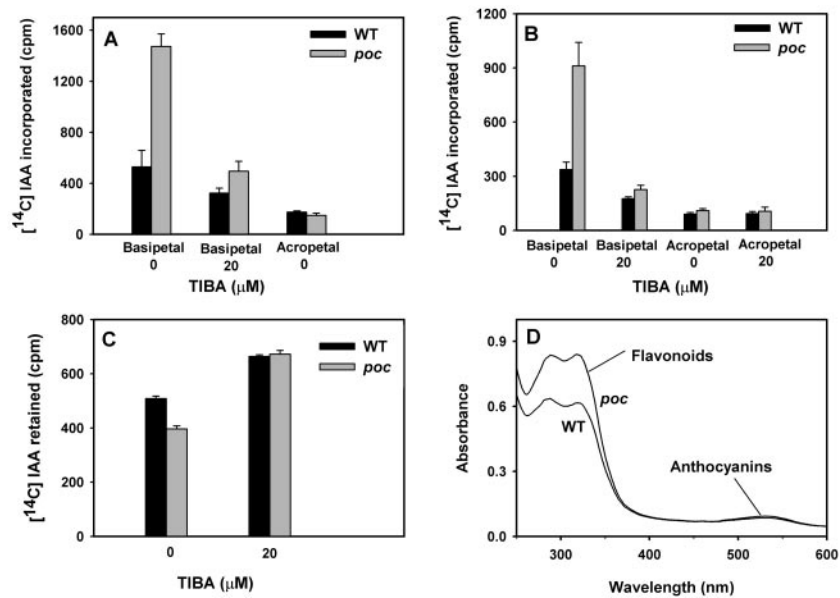


Figure 4. Auxin polar transport in the presence or absence of TIBA. A, Auxin polar transport was measured using the method of Okada et al. (1991) in stem sections of 5-week-old light-grown plants. The basal end of stem segments was submerged in a solution containing [^{14}C] IAA in an Eppendorf tube (Eppendorf Scientific, Westbury, NY) and after 4 h, a 5-mm section from non-submerged end of segments was excised, and the amount of radioactivity was determined. Error bars = SE of five replicates. B, Auxin polar transport was measured using the method of Daniel et al. (1989) in stem sections of 4-week-old light-grown plants. The stem segments were sandwiched on glass microscopic slides between the receiver and donor blocks of agar, and the setup was placed vertically in a humid chamber. After 4 h of incubation, the amount of radioactivity was counted in the receiver blocks. Error bars = SE of five replicates. C, Auxin efflux rate was measured by the retention of the amount of [^{14}C] IAA in the hypocotyls of 3-week-old light grown plants. The cut segments of hypocotyls were floated on a solution containing [^{14}C] IAA either with or without TIBA. Then, segments were incubated for another 2 h in the same buffer without IAA/TIBA and counted for radioactivity. Error bars = SE of five replicates. D, Absorption spectrum of flavonoids extracted from stems of 4-week-old light-grown *poc* and wild-type plants.

Enhanced PAT Alters Gravitropic Curvatures

The experiments on the rescue of the *poc* phenotype and auxin action on organ elongation indicated that enhanced PAT may cause depletion of auxin in hypocotyl tissue and at the same time may cause over accumulation of auxin at the root tip. Such alteration in auxin level is expected to affect physiological processes such as gravitropic curvature that are related to auxin levels or distribution. Therefore, we compared gravitropic curvature of the hypocotyl and of the root in the *poc* mutant with that in wild type. The gravitropic curvature of the *poc* hypocotyl differed from wild type in two aspects (Fig. 7A). First, onset of curvature in *poc* seedlings could be seen only after a lag period of 1 h, which was almost twice that required for wild type. Second, at all time points, the magnitude of curvature was much lower than that for wild-type seedlings. In fact, some *poc* seedlings showed only a little curvature even after 5 h of gravistimulation. However, after 24 h, these *poc* seedlings showed significant curvature, albeit the extent of the curvature in *poc* seedlings was less than in the wild type.

It is believed that curvature of the root tip on gravistimulation results from basipetal flow of auxin from the root tip into cortical and epidermal cells. In

that case, accumulation of auxin at the root tip due to enhanced PAT in the mutant would be expected to increase the amount of basipetal flow of auxin leading to higher curvatures. For *poc* seedlings, a higher root gravitropic curvature was observed compared with wild type (Fig. 7B). Interestingly, the gravitropic curvature of roots of the *poc* mutant showed deviation from wild type in two aspects in an entirely opposite way from that seen for the hypocotyl. First, the lag period of curvature in *poc* was reduced to 10 min compared with a lag of 15 min in wild type. Second, for *poc*, a much higher degree of curvature was seen compared with wild type.

DISCUSSION

Phenotypes Exhibited by *poc* Mutant Are Most Likely Caused by an Increase in Polar Transport of Auxin

The strong pleiotropic effect of the *poc* mutation lasting throughout the plant life cycle likely signifies modification in some central physiological processes regulating plant development. The observed developmental abnormalities in the *poc* mutant such as increase in cotyledon numbers, change in shape and size of the leaf, loss of lobing in the leaflet, ectopic formation of organs on the rachis, increased number

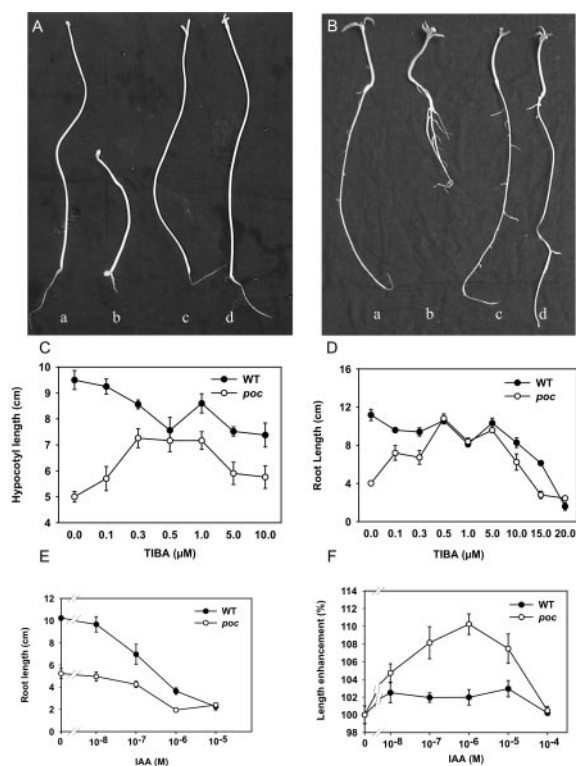


Figure 5. Hypocotyl and root growth of seedlings in the presence of TIBA and IAA. A, Morphology of 9-d-old dark-grown wild-type (a and c) and *poc* (b and d) seedlings in the presence (c and d) or absence (a and b) of TIBA ($0.5 \mu\text{M}$). B, Morphology of 9-d-old light-grown wild-type (a and c) and *poc* (b and d) seedlings in the presence (c and d) or absence (a and b) of TIBA ($0.5 \mu\text{M}$). C, Effect of various concentrations of TIBA on elongation of hypocotyl length of 10-d-old dark-grown *poc* seedlings compared with the wild type. D, Effect of various concentrations of TIBA on elongation of root lengths of 9-d-old light-grown *poc* seedlings compared with wild type. E, Effect of various concentrations of IAA on root elongation of 9-d-old light-grown wild-type seedlings compared with *poc*. F, Effect of IAA in promoting elongation of hypocotyl segments of 5-d-old dark-grown *poc* seedlings compared with wild type.

of flowers in the inflorescence, and fusion of floral organs are broadly reminiscent of alteration in phytohormone action. Examination of mutant seedlings revealed a 3-fold higher level of PAT. During postembryonic development, interference with PAT by mutation or exogenous application of PAT inhibitors results in defects in leaf morphology and venation, inflorescence architecture, vascular anatomy, and tropic movement of plants (Friml and Palme, 2002). Interestingly, several of the morphological and anatomical changes in the *poc* mutant are the reverse of those observed for Arabidopsis mutants such as *pin1* (Okada et al., 1991; Gälweiler et al., 1998), *tir3* (Ruegger et al., 1997), and *ifl1* (Zhong and Ye, 2001) that display a reduction in PAT. The stronger alleles of these mutants develop a pin-shaped inflorescence devoid of floral primordia and abnormal leaves. In contrast, the *poc* mutant shows features such as ex-

tensive branching of the inflorescence with numerous abnormal flowers (Fig. 1).

Several lines of evidence indicate that developmentally regulated auxin levels and distribution specify vascular differentiation during normal plant organogenesis (Ye, 2002). Such a role for auxin as an inducer of vascular differentiation is seen in auxin-overproducing transgenic plants, wherein an excess of auxin levels causes increase in the amounts of vascular tissue (Klee et al., 1987). PAT is essential for the formation of spatially organized patterns of vascular tissue, and a reduction of PAT in *ifl1* and *pin1* mutants is accompanied by proliferation of xylem in the vascular bundles of inflorescence stems (Gälweiler et al., 1998; Mattsson et al., 1999; Tsiantis et al., 1999; Zhong and Ye, 2001). Because reduction in PAT increases vascular proliferation, increase in PAT is expected to reduce auxin levels in the stem and display the opposite effect. In fact, auxin-deficient transgenic plants show a reduction in vascular development (Romano et al., 1991). The anatomical alterations observed in *poc*, such as smaller epidermal cells and compact placement of vascular bundles with reduction of the central pith (Fig. 6), are in conformity with the view that these changes may reflect reduced auxin levels due to increase in PAT.

One way to ascertain a causal connection between the mutation and a physiological process is to phenocopy the mutation by external application of bioactive molecules. In several instances, phenotypes of mutants defective in PAT have been phenocopied in wild type by application of PAT inhibitors (Okada et al., 1991; Gälweiler et al., 1998). Although a lack of agonists that can stimulate PAT in plants precludes phenocopy of the *poc* mutation in wild type, we tested whether the application of PAT inhibitors to the *poc* mutant could rescue the mutant phenotype to wild type. Etiolated seedlings of the *poc* mutant characteristically show a shorter hypocotyl, whereas the light-grown mutant seedlings exhibit a shorter primary root than the wild type. A rescue of the phenotype is clearly seen in seedlings raised in the presence of TIBA (Fig. 5). TIBA increases the root and hypocotyl lengths of the mutant seedlings to close to that of the wild type. A similar rescue of phenotype by TIBA was also seen for anatomical alteration in the *poc* mutant. Taken together, we can reasonably speculate that the aberrant morphology of the *poc* mutant may be induced by an enhancement in PAT.

Several lines of evidence support the assumption concerning elevation in the rate of auxin transport in the *poc* mutants. First, direct quantification of basipetal transport shows that the rate of auxin transport in the *poc* mutant is nearly 3-fold higher than in the wild type, and the exogenous application of TIBA reduces the transport rate close to the wild-type control. Second, tomato stems preloaded with radiolabeled auxin show a higher rate of auxin efflux in the *poc* mutant compared with wild type. Again, in this case,

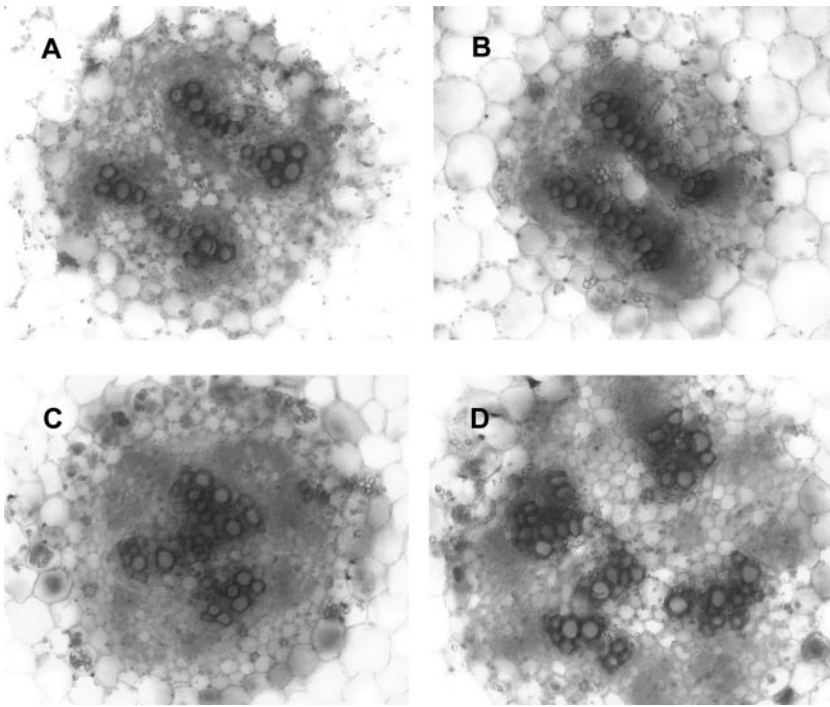


Figure 6. Transverse sections showing the vasculature in hypocotyls of 15-d-old light-grown *poc* seedlings in the presence or absence of TIBA (10 μM). Sections were taken from the middle portion of hypocotyls and stained with safranin. A, Wild type; B, wild type + TIBA; C, *poc* mutant; D, *poc* mutant + TIBA. Note the difference in placement of the vascular bundles between mutant and wild type. Scale bars in A to D: 50 μm .

TIBA reduces the efflux rate in the mutant to the levels observed for wild type. The auxin transport in inflorescence stems and hypocotyls of the flavonoid-deficient *tt4* mutant is elevated over wild type by about 2-fold (Brown et al., 2001). The observed increase in PAT in the *poc* mutant cannot be explained by a general reduction in the levels of flavonoids because the mutant plants had nearly the same level of flavonoids as in the wild type. Together, these data strengthen the view that the *poc* mutation enhances the rate of auxin transport, and it acts at a step other than flavonoid biosynthesis.

Enhanced Auxin Polar Transport Likely Alters Auxin Distribution Pattern in the *poc* Mutant

Auxin distribution has been implicated as a key regulator of several developmental processes such as cell elongation and tropic curvatures. Mutations affecting PAT in several instances may elicit their phenotype by consequent disturbance of the auxin balance of the tissues (Sabatini et al., 1999). Etiolated hypocotyls of *mdr1* mutants, defective in PAT, display larger gravitropic and phototropic curvatures probably due to accumulation of auxin (Spalding et al., 2002). On the contrary, increase in PAT may result in faster removal of auxin, reducing its lateral flow. One critical physiological assay for the lateral flow of auxin is the magnitude of gravitropic curvature that is related to its lateral distribution as per Cholodny and Went's hypothesis (Trewavas, 1992). The decrease in the lateral flow of auxin in the *pin3* mutant also correlates with a reduction in the tropic curvature of *Arabidopsis* seedlings (Friml et al.,

2002b). The observed delay in onset and reduction in magnitude of gravitropic curvature in *poc* hypocotyls is consistent with reduction in auxin levels in the tissue due to enhanced PAT. Reduced lateral flow of auxin also correlates with a reduction in the width of epidermal cells in *poc* hypocotyls. The paucity of auxin in hypocotyls is also indicated by greater stimulation of hypocotyl elongation by auxin in the *poc* mutant than wild type and is consistent with its depletion due to increased PAT.

One of the obvious consequences of enhanced PAT is the likelihood of channelization of most auxin to the root pole, causing its accumulation at the root tip. Three lines of evidence point to such an overaccumulation in the *poc* mutant based on current physiological models of auxin-mediated root growth and tropic curvature (Sabatini et al., 1999; Masson et al., 2002). First, a reduction in the root tip growth observed is consistent with an increased level of auxin because beyond a threshold level, auxin acts as an inhibitor of growth. In fact, such accumulation of auxin at the root tip in transgenic *pinoid*-overproducing plants leads to total collapse of the root meristem, and this could be rescued by application of PAT inhibitors (Benjamins et al., 2001). An increase in root length of *poc* seedlings by application of PAT inhibitors indicates that the increased accumulation of auxin may be responsible for the decreased root growth. Second, adult *poc* plants produce more lateral roots than the wild type (Reed et al., 1998). Third, an increased accumulation of auxin at the root meristem would also increase the "back flow" of auxin in the basipetal direction in epidermal and cortical cells of the root. Such increase in the

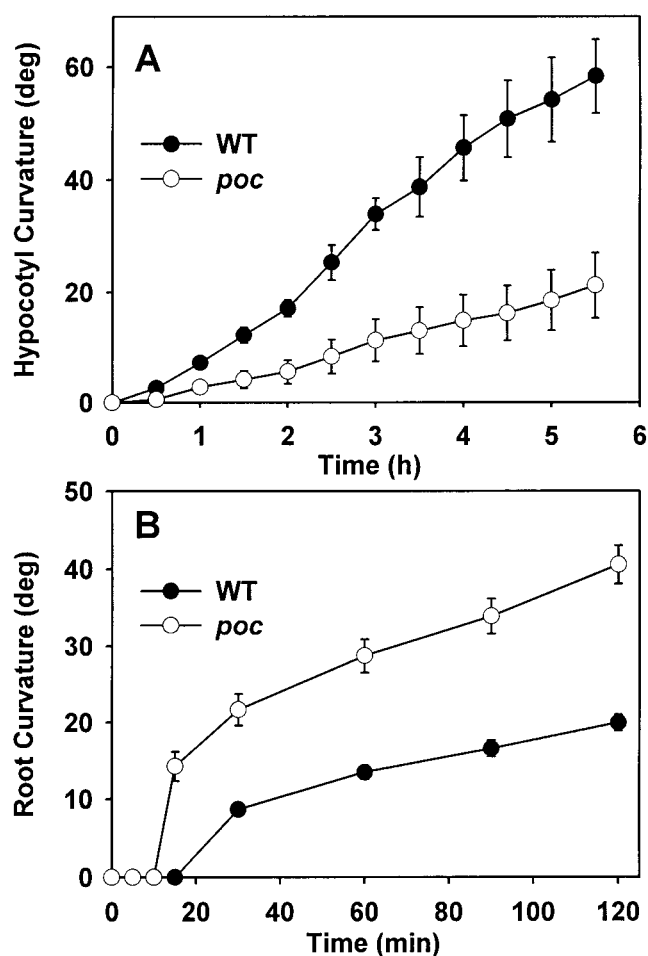


Figure 7. Analysis of gravitropic response in seedlings. A, Kinetics of gravitropic response in the hypocotyls of 7-d-old light-grown wild-type and *poc* seedlings. Seedlings grown in plastic cuvettes were reoriented 90° relative to the gravity vector. The curvature was determined by photographing the seedlings at the given time intervals using a PC camera. B, Gravitropic response in the roots of 1-d-old light-grown wild-type and *poc* seedlings. Seedlings grown on vertical agar plates were reoriented 90° relative to the gravity vector. The curvature was determined by photographing the roots at the given time intervals using a PC camera.

basipetal flow of auxin in the root, as per the “fountain model” of auxin-mediated root gravitropism, would be predicted to stimulate the gravitropic root tip curvature in the *poc* mutant. Analysis of root gravitropic curvature broadly substantiates this view because gravistimulated *poc* root tips showed a much shorter lag period and nearly twice the curvature compared with wild type.

Is Polar Transport of Auxin Related to Initiation of Cotyledons in the Globular Embryo?

Auxin is considered as a principal regulator of patterning during embryogenesis. Because auxin is polarly transported and may act in a non-cell autonomous fashion, it can provide the necessary input for

determination of pattern specificity (Souter and Lindsey, 2000; Berleth and Chatfield, 2002). Recent reports have brought some support to the role of auxin as a “morphogen” regulating cell differentiation in a concentration-dependent manner (Sabatini et al., 1999; Friml et al., 2002a). Current research on embryo development in *Arabidopsis* mutants has highlighted that the transition from the globular to the heart stage requires elements participating in auxin perception and distribution. A role for auxin in the progression of embryogenesis is indicated by the observation that a null mutation in the auxin-binding protein *ABP1* arrests *Arabidopsis* embryogenesis at the globular stage (Chen et al., 2001). Similarly, failure to establish a properly localized distribution of auxin transporting proteins during the globular stage in the *gnom* mutant results in an abnormal embryo devoid of cotyledonary primordia (Mayer et al., 1993; Steinmann et al., 1999).

The appearance of cotyledonary poles on a developing embryo marks the end of the globular stage leading to establishment of bilateral symmetry. Available evidence indicates that development of the auxin transport system during the globular stage is related to the subsequent appearance of cotyledon primordia. In a range of plant species, disruption of PAT either by a mutation such as *pin1* (Liu et al., 1993) or *gnom* (Mayer et al., 1993) or by using inhibitors of auxin transport during zygotic and also somatic embryogenesis (Hadfi et al., 1998; Liu et al., 1993) disrupts embryonic development with generation of embryos with fused or missing cotyledons. Thus, normal auxin transport appears to be one of the prerequisites for the radial globular embryo to progress to the bilaterally symmetrical heart stage embryo (Liu et al., 1993; Hadfi et al., 1998). However, our knowledge about the events leading to onset of cotyledon initiation during embryogenesis is limited. Embryonic fate mapping using chimeric tissue indicated that in *Arabidopsis*, first one cotyledon gets determined and that in turn directs the positioning of the other cotyledon at the opposite end. It is suggested that some kind of lateral inhibition is responsible for this process, directing the formation of new primordia at the site of lowest inhibition (Woodruff et al., 2000).

The association of defects in auxin transport with alterations in cotyledon initiation/separation in a number of instance points to the likelihood of auxin playing an important role in the initiation of cotyledon development. Based on reports that indicate association between auxin transport and cotyledon development, it seems possible that faster removal of auxin may result in initiation of additional cotyledons. In fact, based on their results on auxin and PAT inhibitor application to developing mustard embryos, Hadfi et al. (1998) proposed that polar transport removes auxin from the area between the two emerging cotyledon primordia causing separation of cotyledons. Therefore, the removal of auxin by en-

hanced polar transport could deplete auxin below a threshold level in cells of the apical dome, leading to initiation of additional cotyledon primordia. The appearance of multiple cotyledons in *poc* embryos at the transition from globular to heart stage is indicative of such a link between auxin transport and cotyledon formation. Likewise, the reduction in size of epidermal cells in *poc* embryos compared with wild type could be a consequence of increased PAT.

Though an association of increase in cotyledon number with increase in PAT is seen for the *poc* mutant of tomato, it is at variance with the *pinoid* mutant of Arabidopsis, which shows polycot seedlings but reduced PAT in inflorescence stems (Bennett et al., 1995). A recent report suggested that *PI-NOID* acts as a positive regulator of PAT (Benjamins et al., 2001), whereas our results indicate *POC* to be a negative regulator. It is proposed that *PINOID* may be required for proper positioning of cotyledonary primordia (Benjamins et al., 2001), whereas *POC* action might be related to separation of cotyledon primordia (Hadfi et al., 1998). In such a case, these two might affect different physiological processes and still show similar phenotypic effects. It could be equally plausible that enhanced PAT in Arabidopsis is not related to development of polycotyly. For example, the Arabidopsis *tt4* mutant shows enhanced PAT but does not exhibit a polycot phenotype (Brown et al., 2001).

In summary, our results indicate that the *poc* mutation of tomato shows increased PAT and that this could be responsible for its pleiotropic phenotype. We have located the *poc* gene on chromosome nine of tomato (M. Kavitha, P. Bauer, M.S. Sharada, A.S.A. Al-Hammadi, P. Janila, S. Negi, R. Sharma, unpublished data) and are currently fine mapping it with an aim to isolate and determine its role in PAT.

MATERIALS AND METHODS

Plant Growth Conditions

Tomato (*Lycopersicon esculentum* L. cv Ailsa Craig) seeds were surface sterilized and sown on filter papers. After emergence of the radicle, seedlings were grown on vermiculite either under continuous white light ($100 \mu\text{mol m}^{-2} \text{s}^{-1}$) or in darkness at 25°C. Unless otherwise mentioned, for all experiments the plant age was counted from the time point of emergence of the radicle. To test the viability, pollens were germinated on Brewbaker and Kwack's media (Brewbaker and Kwack, 1963), and the percentage pollen germination was calculated after staining with 1% (w/v) acetocarmine. Leaf and cotyledon venation was examined by depigmenting tissues in acidified methanol (2% [v/v] HCl) followed by clearing in a mixture of chloral hydrate:glycerol:water (8:1:2 [w/v]) and staining with *p*-rosaniline hydrochloride. Flavonoid content of 4-week-old light-grown plants ($n = 10$, three replicates) was estimated according to Harborne (1967). The shoots of these plants were excised and extracted in 10 mL of acidified (1% [v/v] HCl) methanol for 24 h in darkness with shaking. After centrifugation, the absorption spectra were recorded. The total flavonoid level is expressed as A_{330}/shoot . The experimental data for the cell size and morphological variation was also analyzed by a two-tailed Student's *t* test, and *P* values were calculated.

Mutants Screening and Genetic Analysis

The ethyl methanesulfonate (EMS) mutagenesis was performed essentially following the procedure of Koornneef et al. (1990). Approximately 5,000 seeds of tomato cv Ailsa Craig were soaked in a solution of 60 mM EMS for 24 h in the dark at room temperature. Thereafter, the seeds were washed with distilled water, and M_1 generation plants were grown in the field. From fruits of a population of approximately 1,500 M_1 plants, M_2 seeds were harvested in bulk. A population of approximately 50,000 EMS-mutagenized M_2 seedlings was screened for putative cotyledon mutants. One-week-old seedlings were screened for altered cotyledon number and size. Of 25 putative mutants showing multiple cotyledons, only nine mutants survived. Because the mutants were male sterile, these were rescued by manually pollinating with wild-type pollens, and F_1 heterozygous seeds were obtained. Subsequently, mutants were also manually self-pollinated, and homozygous seeds were obtained. The complementation analysis using isolated mutant lines indicated that all nine mutants were allelic. For all experiments, seeds multiplied from the mutant line *poc1-1* that was backcrossed twice were used.

Embryogenesis

Both the wild-type and *poc* mutant flowers were emasculated and manually self-pollinated. The developing fruits were harvested at regular intervals starting 10 DAP. Pistils were removed from the developing fruits and fixed in ethanol:acetic acid (6:1 [v/v]) overnight. After several washes in 100% ethanol followed by washing in 70% ethanol, the pistils were preserved in 70% ethanol. The pistils were then cleared in a mixture of chloral hydrate:glycerol:water (8:1:2 [w/v]) overnight (Berleth and Jurgens, 1993) and dissected under a dissection microscope to reveal the ovules, which were then further dissected to remove embryos. The embryos were observed using a Zeiss Axiophot microscope under DIC optics (Zeiss, Oberkochen, Germany) and photographed using black and white film (15-25 ASA; Siddiqi et al., 2000).

PAT Assay

The polar transport of auxin was assayed in the stem segments of light-grown plants using two different protocols outlined by Okada et al. (1991) and Daniel et al. (1989) with some modifications. The height and the diameters of the stems of both *poc* and wild-type plants were nearly similar. For the Okada et al. (1991) protocol, 10 stem segments (2.5 cm) were cut 2 mm below the cotyledonary node from 5-week-old light-grown plants. The segments were first floated for 2 h in 5 mM phosphate buffer (pH 5.8) containing either 1 μM IAA or 20 μM TIBA. To avoid a gravitropic response during that period, this pre-incubation took place on a shaker. Thereafter, either the apical or basal end of the segments (for basipetal or acropetal transport, respectively) was submerged in 50 μL of 5 mM phosphate buffer (pH 5.8) with 27 nCi mL^{-1} (specific activity = 4.2 mCi mmol^{-1} of [$1,2\text{-}^{14}\text{C}$] IAA; BRIT, Mumbai, India) and 1 μM IAA (unlabeled) in a 1.5-mL Eppendorf tube. After 4 h, a 5-mm section from the non-submerged end of segments was excised and floated overnight in 3 mL of Bayer's solution. The radioactivity was counted in a Beckman liquid scintillation counter. Similar to Brown et al. (2001), we also found that a 4-h transport period was sufficient to measure PAT in tomato, unlike 18 h used by Okada et al. (1991).

For the Daniel et al. (1989) protocol using agar blocks, stem segments (1.2 cm) of 4-week-old tomato plants were excised 2 mm below the cotyledonary node and incubated for 2 h in 5 mM phosphate buffer (pH 5.8) containing either 1 μM IAA or 20 μM TIBA on a shaker. These segments were sandwiched on glass microscopic slides between receiver (1.5% [w/v] agar in water, $2.5 \times 0.4 \times 0.4$ cm) and donor blocks (1.5% [w/v] agar in 5 mM phosphate buffer [pH 5.8] containing 1 μM IAA and approximately 17 nCi mL^{-1} [^{14}C -IAA], $2.5 \times 0.8 \times 0.4$ cm). Twelve segments for each of the donor receiver block units were placed either in basipetal (apical end toward donor block) or in acropetal direction (with basal end toward donor). The donor receiver block units were placed vertically in a humid chamber at 25°C \pm 2°C, and the system was inverted to prevent drainage of [^{14}C IAA] onto the receiver blocks. After 4 h of incubation, the receiver blocks were removed and placed in 3 mL of liquid scintillation cocktail. The samples were shaken at 100 rpm for 2 h and left overnight at 25°C \pm 2°C before counting in a scintillation counter.

Auxin Efflux Assay

Auxin efflux in the hypocotyls was assayed according to the procedure of Bernasconi (1996). Twelve hypocotyls of 3-week-old light-grown seedlings were cut into segments (4 mm). The segments were floated with shaking for 2 h in 5 mM phosphate buffer (pH 5.8) with 1% (w/v) Suc containing 0.1 $\mu\text{Ci mL}^{-1}$ [^{14}C] IAA either with or without 20 μM TIBA. Then, the segments were rinsed and incubated for another 2 h in the same buffer without IAA/TIBA. After a final rinse, the segments were placed in Bayer's solution and counted for radioactivity as described above.

Effect of TIBA on Organ Elongation

Surface-sterilized seeds of tomato were germinated in the dark. After the emergence of the radicle, seeds were transferred either onto petri plates or germination boxes containing 1.7% (w/v) agar support prepared with one-tenth-strength Murashige and Skoog media (inorganic salts only, Murashige and Skoog, 1962). For studying the effect of TIBA on root length, seeds were sown on agar containing different concentrations of TIBA in the range of 0 to 20 μM . The petri plates were vertically oriented after 9-d seedlings were removed, and the root lengths were measured. To study the effect of TIBA on hypocotyl length, seeds were sown on 1.7% (w/v) agar in transparent germination boxes containing different concentrations of TIBA in the range of 0 to 20 μM . The germination boxes were kept in the dark for 10 d. On the 10th d, the hypocotyl lengths were measured.

Effect of Auxin on Organ Elongation

The method of estimating elongation of hypocotyls was essentially similar to that described earlier by Kelly and Bradford (1986), with the variation that the hypocotyls were used immediately after excision and were not depleted of endogenous auxin. One-centimeter segments of hypocotyls were excised from 5-d-old dark-grown seedlings and floated in 5 mM phosphate buffer (pH 5.8) containing 1% (w/v) Suc with and without 1 μM IAA. The length of each segment was recorded after 4 h. For study on root length, seedlings were grown on agar with or without IAA in the light on vertical petri plates, and the root lengths were measured after 9 d.

SEM

The middle region from hypocotyls and cotyledons of 7-d-old light-grown seedlings was excised and mounted on stubs using a double-sided adhesive tape. In the case of cotyledons, the abaxial side was examined for epidermal cell shape. The stubs were plunged in liquid nitrogen, and the frozen organs were immediately examined in an environmental scanning electron microscope (Philips, Eindhoven, The Netherlands).

Light Microscopy

Free-hand sections were cut from the hypocotyls of 15-d-old light-grown seedlings. At this age, hypocotyls were approximately 3.5 cm long. The sections were cut from at least 10 seedlings from the central region of hypocotyls at a distance of 1.5 to 2 cm from the cotyledonary node. The cut sections were immediately stained in safranin and were destained in water. The sections were mounted on slides in water and were photographed in a Zeiss Axiophot microscope using DIC optics.

Analysis of Gravitropism

Gravity response in the hypocotyls was measured using 7-d-old light-grown seedlings grown vertically in plastic cuvettes filled with vermiculite. At the time of gravistimulation, seedlings were turned 90°, and the cuvettes were arranged in a rack. Seedlings were photographed using an Ezonics (Ezcam) PC camera (Ezonics Corporation, Pleasanton, CA) at every 15-min interval initially and later at every 30 min for 6 h. For each experiment, five *pac* and five wild-type seedlings were used and the experiment was repeated six to eight times. The angles were measured using Image Tool program after subtracting the zero time point image from the image at required time points.

For root gravitropism, seeds with just emerged radicles were sown on 1.7% (w/v) agar in petri plates, and plates were kept vertically under continuous white light. After 24 h, when roots elongated to 5 to 6 mm, the plates were rotated by 90°, and images were recorded at every 5 min for 2 h using an Ezonics PC camera. Each petri plate had three *pac* and three wild-type seedlings, and the experiment was repeated about 10 times.

ACKNOWLEDGMENTS

We wish to thank Dr. Bernie Carroll (University of Queensland, Australia) for providing us the *dem* mutant seeds, Dr. Shashi Singh (Centre for Cellular and Molecular Biology, Hyderabad, India) for light microscopy, and Dr. Manjunath (Central Instruments Laboratory, University of Hyderabad, Hyderabad, India) for SEM.

Received April 15, 2003; returned for revision May 18, 2003; accepted May 24, 2003.

LITERATURE CITED

- Benjamins R, Quint A, Weijers D, Hooykaas P, Offringa R (2001) The PINOID protein kinase regulates organ development in *Arabidopsis* by enhancing polar auxin transport. *Development* **128**: 4057–4067
- Bennett MJ, Marchant A, Green HG, May ST, Ward SP, Millner PA, Walker AR, Schulz B, Feldmann KA (1996) Arabidopsis AUX1 gene: a permease like regulator of root gravitropism. *Science* **273**: 948–950
- Bennett SRM, Alvarez J, Bossinger G, Smyth DR (1995) Morphogenesis in *pinoid* mutants of *Arabidopsis thaliana*. *Plant J* **8**: 505–520
- Berleth T, Chatfield S (2002) Embryogenesis: pattern formation from a single cell. In CR Somerville, EM Meyerowitz, eds, *The Arabidopsis Book*. American Society of Plant Biologists, Rockville, MD, <http://www.aspb.org/downloads/arabidopsis/berleth.pdf>
- Berleth T, Jurgens G (1993) The role of the *monopteros* gene in organizing the basal body region of the *Arabidopsis* embryo. *Development* **118**: 575–587
- Bernasconi P (1996) Effect of synthetic and natural protein tyrosine kinase inhibitors on auxin efflux in zucchini (*Cucurbita pepo*) hypocotyls. *Plant Physiol* **96**: 205–210
- Bernasconi P, Bhavesh CP, Reagan JD, Subramanian MV (1996) The N-1-naphthylphthalamic acid-binding protein is an integral membrane protein. *Plant Physiol* **111**: 427–432
- Brewbaker JL, Kwack BH (1963) The essential role of calcium ion in pollen germination and pollen tube growth. *Am J Bot* **50**: 859–865
- Brown DE, Rashotte AM, Murphy AS, Normanly J, Tague BW, Peer WA, Taiz L, Muday GK (2001) Flavonoids act as negative regulators of auxin transport in vivo in *Arabidopsis*. *Plant Physiol* **126**: 524–535
- Chen J-G, Ullah H, Young JC, Sussman MR, Jones AM (2001) ABP1 is required for organized cell elongation and division in *Arabidopsis* embryogenesis. *Genes Dev* **15**: 902–911
- Chen R, Hilson P, Sedbrook J, Rosen E, Caspar T, Masson PH (1998) The *Arabidopsis thaliana* AGRVITROPIC 1 gene encodes a component of the polar-auxin-transport efflux carrier. *Proc Natl Acad Sci USA* **95**: 15112–15117
- Christensen SK, Dagenais N, Chory J, Weigel D (2000) Regulation of auxin response by the protein kinase PINOID. *Cell* **100**: 469–478
- Coenen C, Christian M, Lüthen H, Lomax TL (2003) Cytokinin inhibits a subset of *diageotropica*-dependent primary auxin responses in tomato. *Plant Physiol* **131**: 1692–1704
- Daniel SG, Rayle DL, Cleland RE (1989) Auxin physiology of tomato mutant *diageotropica*. *Plant Physiol* **91**: 804–807
- Friml J, Palme K (2002) Polar auxin transport—old questions new concepts? *Plant Mol Biol* **49**: 273–284
- Friml J, Benková E, Blilou I, Wisniewska J, Hamann T, Ljung K, Woody S, Sandberg G, Scheres B, Jürgens G et al. (2002a) AtPIN4 mediates sink-driven auxin gradients and root patterning in *Arabidopsis*. *Cell* **108**: 661–673
- Friml J, Wisniewska J, Benková E, Mendgen K, Palme K (2002b) Lateral relocation of auxin efflux regulator PIN3 mediates tropism in *Arabidopsis*. *Nature* **415**: 806–809
- Gälweiler L, Guan C, Müller A, Wisman E, Mendgen K, Yephremov A, Palme K (1998) Regulation of polar auxin transport by AtPIN1 in *Arabidopsis* vascular tissue. *Science* **282**: 2226–2230

- Geldner N, Anders N, Wolters H, Keicher J, Kornberger W, Muller P, Delbarre A, Ueda T, Nakano A, Jurgens G (2003) The Arabidopsis GNOM ARF-GEF mediates endosomal recycling, auxin transport, and auxin-dependent plant growth. *Cell* **112**: 219–230
- Geldner N, Friml J, Stierhof Y-D, Jurgens G, Palme K (2001) Auxin transport inhibitors block PIN1 cycling and vesicle trafficking. *Nature* **413**: 425–428
- Gil P, Dewey E, Friml J, Zhao Y, Snowden KC, Putterill J, Palme K, Estelle M, Chory J (2001) BIG: a calossin-like protein required for polar auxin transport in *Arabidopsis*. *Genes Dev* **15**: 1985–1997
- Hadfi K, Speth V, Neuhaus G (1998) Auxin-induced developmental patterns in *Brassica juncea* embryos. *Development* **125**: 879–887
- Harborne JB (1967) Comparative Biochemistry of Flavonoids. Academic Press, London
- Jacobs M, Gilbert SF (1983) Basal localization of the presumptive auxin transport carrier in pea stem cells. *Science* **220**: 1297–1300
- Jacobs M, Rubery PH (1988) Naturally occurring auxin transport regulators. *Science* **241**: 346–349
- Keddie JS, Carroll BJ, Thomas CM, Reyes MEC, Klimyuk V, Holtan H, Gruissem W, Jones JDG (1998) Transposon tagging of the defective embryo and meristems gene of tomato. *Plant Cell* **10**: 877–888
- Kelly MO, Bradford KJ (1986) Insensitivity of the *diageotropica* tomato mutant to auxin. *Plant Physiol* **82**: 713–717
- Klee HJ, Horsch RB, Hinchee MA, Hein MB, Hoffmann NL (1987) The effects of overproduction of two *Agrobacterium tumefaciens* T-DNA auxin biosynthetic gene products in transgenic petunia plants. *Genes Dev* **1**: 86–96
- Koornneef M, Bosma TDG, Hanhart CJ, Van der Veen JH, Zeevaart JAD (1990) The isolation and characterization of gibberellin-deficient mutants in tomato. *Theor Appl Genet* **80**: 852–857
- Liu C-M, Xu Z-H, Chua N-H (1993) Auxin polar transport is essential for the establishment of bilateral symmetry during early plant embryogenesis. *Plant Cell* **5**: 621–630
- Lomax TL, Muday GK, Rubery PH (1995) Auxin transport. In PJ Davies, ed, Plant Hormones, Physiology, Biochemistry and Molecular Biology. Kluwer Academic Publishers, Dordrecht, The Netherlands, pp 509–530
- Luschnig C, Gaxiola RA, Grisafi P (1998) Fink GR EIR1 a root-specific protein involved in auxin transport is required for gravitropism in *Arabidopsis thaliana*. *Genes Dev* **12**: 2175–2187
- Marchant A, Kargul J, May ST, Muller P, Delbarre A, Perrot-Rechenmann C, Bennett MJ (1999) AUX1 regulates root gravitropism in *Arabidopsis* by facilitating auxin uptake within root apical tissues. *EMBO J* **18**: 2066–2073
- Masson PH, Tasaka M, Morita MT, Guan C, Chen R, Boonsirichai K (2002) *Arabidopsis thaliana*: a model for the study of root and shoot gravitropism. In CR Somerville, EM Meyerowitz, eds, The Arabidopsis Book. American Society of Plant Biologists, Rockville, MD, <http://www.aspb.org/downloads/arabidopsis/masson.pdf>
- Mattsson J, Sung ZR, Berleth T (1999) Responses of plant vascular systems to auxin transport inhibition. *Development* **126**: 2979–2991
- Mayer U, Buettner G, Jurgens G (1993) Apical-basal pattern formation in the *Arabidopsis* embryo: studies on the role of the *gnom* gene. *Development* **117**: 149–162
- Muday GK, Brunn SA, Haworth P, Subramanian M (1993) Evidence for a single naphthylphthalamic acid binding site on the zucchini plasma membrane. *Plant Physiol* **103**: 449–456
- Muday GK, Lomax TL, Rayle DL (1995) Characterization of the growth and auxin physiology of roots of the tomato mutant *diageotropica*. *Planta* **195**: 548–553
- Müller A, Guan C, Gälweiler L, Tanzler P, Huijser P, Marchant A, Parry G, Bennett M, Wisman E, Palme K (1998) AtPIN2 defines a locus of *Arabidopsis* for root gravitropism control. *EMBO J* **17**: 6903–6911
- Murashige T, Skoog F (1962) A revised medium for rapid growth and bioassays with tobacco tissue culture. *Physiol Plant* **15**: 493–497
- Murphy A, Peer WA, Taiz L (2000) Regulation of auxin transport by aminopeptidases and endogenous flavonoids. *Planta* **211**: 315–324
- Okada K, Ueda J, Komaki MK, Bell CJ, Shimura Y (1991) Requirement of the auxin polar transport system in early stages of *Arabidopsis* floral bud formation. *Plant Cell* **3**: 677–684
- Pickett FB, Wilson AK, Estelle M (1990) The *aux1* mutation of *Arabidopsis* confers both auxin and ethylene resistance. *Plant Physiol* **94**: 1462–1466
- Rashotte AM, DeLong A, Muday GK (2001) Genetic and chemical reductions in protein phosphatase activity alter auxin transport gravity response and lateral root growth. *Plant Cell* **13**: 1683–1697
- Raven J (1975) Transport of indoleacetic acid in plant cells in relation to pH and electric potential gradients, and its significance for polar IAA transport. *New Phytol* **74**: 163–172
- Reed RC, Brady SR, Muday GK (1998) Inhibition of auxin movement from the shoot into the root inhibits lateral root development in *Arabidopsis*. *Plant Physiol* **118**: 1369–1378
- Romano CP, Hein MB, Klee HJ (1991) Inactivation of auxin in tobacco transformed with the indole acetic acid-lysine synthetase gene of *Pseudomonas savastanoi*. *Genes Dev* **5**: 438–446
- Rubery PH, Sheldrake AR (1974) Carrier mediated auxin transport. *Planta* **118**: 101–121
- Ruegger M, Dewey E, Hobbie L, Brown D, Bernasconi P, Turner J, Muday G, Estelle M (1997) Reduced naphthylphthalamic acid binding in the *tir3* mutant of *Arabidopsis* is associated with a reduction in polar auxin transport and diverse morphological defects. *Plant Cell* **9**: 745–757
- Sabatini S, Beis D, Wolkenfelt H, Murfett J, Guilfoyle T, Malamy J, Benfey P, Leyser O, Bechtold N, Weisbeek P et al. (1999) An auxin-independent distal organizer of pattern and polarity in the *Arabidopsis* root. *Cell* **99**: 463–472
- Siddiqi I, Ganesh G, Grossniklaus U, Subbaiah V (2000) The *dyad* gene is required for progression through female meiosis in *Arabidopsis*. *Development* **127**: 197–207
- Souter M, Lindsey K (2000) Polarity and signalling in plant embryogenesis. *J Exp Bot* **51**: 971–983
- Spalding E, Murphy A, Noh B (2002) Larger and faster tropisms in *mdr* mutants lacking polar auxin transport. American Society of Plant Biologists, Minisymposium: Tropism. Abs #28003. <http://abstracts.aspb.org/pb2002/public/M16/1053.html>
- Steinmann T, Geldner N, Grebe M, Mangold S, Jackson CL, Paris S, Gälweiler L, Palme K, Jurgens G (1999) Coordinated polar localization of auxin efflux carrier PIN1 by GNOM ARF GEF. *Science* **286**: 316–318
- Trewavas AJ (1992) FORUM: what remains of the Cholodny-Went Theory? *Plant Cell Environ* **15**: 759–794
- Tsiantis M, Brown MIN, Skibinski G, Langdale JA (1999) Disruption of auxin transport is associated with aberrant leaf development in maize. *Plant Physiol* **121**: 1163–1168
- Woodrick R, Martin PR, Birman I, Pickett FB (2000) The *Arabidopsis* embryonic shoot fate map. *Development* **127**: 813–820
- Ye Z-H (2002) Vascular tissue differentiation and pattern formation in plants. *Annu Rev Plant Biol* **53**: 183–202
- Zhong R, Ye Z-H (2001) Alteration of auxin polar transport in the *Arabidopsis ifl1* mutants. *Plant Physiol* **126**: 549–563